

Recent advances in wheel–rail RCF and wear testing

Sundar SHRESTHA^{1,2}, Maksym SPIRYAGIN^{1,2}, Esteban BERNAL^{1,2,*}, Qing WU^{1,2}, Colin COLE^{1,2}

¹ Centre for Railway Engineering, Central Queensland University, Rockhampton 4701, Australia

² Australasian Centre for Rail Innovation, Canberra 2601, Australia

Received: 02 September 2021 / Revised: 09 February 2022 / Accepted: 03 October 2022

© The author(s) 2022.

Abstract: The wear and rolling contact fatigue (RCF) testing approaches for wheels and rails have been reviewed and evaluated in this study. The study points out the advantages and limitations of the existing approaches. The broad analysis revealed that scaled laboratory-based wear testing is widely applied. However, it is necessary to predetermine the input parameters and observing parameters for scaled wear testing for three reasons: first, to emulate the real-world scenarios as closely as possible; second, to postprocess the results received from the scaled testing and transfer them into real practice at full scale; third, to present the results in a legible/appropriate format. Therefore, most of the important parameters required for wear testing have been discussed with fundamental and systematic explanations provided. Additionally, the transition of the parameters from the real-world into the test domain is explained. This study also elaborates on the challenges of the RCF and wear testing processes and concludes by providing major considerations toward successful testing.

Keywords: wear testing; rolling contact fatigue (RCF) testing; wheel–rail

1 Introduction

Wheel and rail interaction plays an important role in the productive operation of the railways. However, the wheel–rail interface is complex because it is an open system with varying external conditions such as diverse wheel and rail geometry, inconsistent displacements and rotational movements of wheels, variable distribution of wheel loads acting on small contact patches, vehicle speed, operational rail self-cleaning mechanism, track irregularities, axle load distributions, and rail vehicle design to name a few. In addition, rail vehicle axle load targets are increasing to attract more financial and operational benefits. To do so, more trains are running on the track, and they are running faster, leading to more damage on the wheel–rail interface.

Thus, the efficient control of impacts on the wheel–rail interface is a crucial aspect of rail vehicle operations. In the wheel–rail interface management, a wear control strategy is one vital part. It is a difficult

problem because measures used to reduce wear (such as application of lubricant) may adversely influence adhesion and fatigue, and measures used to increase adhesion (such as application of sands) may impact on wear. Thus, wear testing is necessary before implementing an effective control strategy to establish a good balance regarding whether to introduce a new lubrication approach and/or more durable wheel or rail materials. There are different approaches to testing and analysing wear in railway operations which will be analytically reviewed in the next section. Also, wear testing is required to generate the wear coefficient to use in the wear simulation model and validate the results from predictive numerical tools. Above all, wheel–rail wear testing delivers the essential insights of the wear mechanism of the combination of particular wheel and rail materials.

2 Wear and RCF relation

In general, wear is a process in which the surface

* Corresponding author: Esteban BERNAL, E-mail: e.bernal@cqu.edu.au

layers of solid bodies are ruptured as a result of their mechanical action against each other [1]. A general classification of different types of wear is presented in Ref. [2]. One such type is wheel–rail wear where the bodies in action are wheels and rails and the mechanical action appears in the form of frictional force [3]. The quantitative definition of wheel–rail wear is the displacement of material from the wheel–rail contact surface. Such wear is influenced by several mechanisms, for instance, presence of friction modifier/enhancer, fluctuating high contact pressure on a varying small contact patch due to different vehicle running conditions, various rolling/sliding speed, etc. Specifically, in the railway industry and academia, there are three widely accepted methods for estimating wheel and rail wear rates [4]: the T-gamma model [5,6], the Archard model developed by British Rail Research [7, 8], and the USFD model from the University of Sheffield [9–11]. The T-gamma approach uses the wheel–rail contact pressure and sliding velocity to determine the energy dissipation from the wheel–rail contact and can be formulated as the T_γ value [12]:

$$T_\gamma = [T_y \gamma_y] + [T_x \gamma_x] + [M_z \omega_z] \quad (1)$$

where T and M are the longitudinal and lateral creep forces and spin creep force components, γ and ω are the longitudinal, lateral, and spin creepage components. Depending on the T_γ value, the wheel–rail wear is categorized into three types: mild, severe, and catastrophic [13]. The first two types occur on the straight track (wheel tread–railhead contact), and the last one may occur on tight curved track (wheel flange–rail gauge contact). The transition from severe to catastrophic occurs during the shift of the contact interface from wheel tread to wheel flange contact. The Archard wear model approach states that the material volume loss (V) is a function of the sliding distance (s), normal force (N), and the material hardness (H) formulated as [12]:

$$V = k \frac{Ns}{H} \quad (2)$$

where k is the wear coefficient, which similarly to the energy dissipation approach, classifies the wear volume loss results as mild, severe, and catastrophic. Finally,

the USFD model expands the T_γ approach in terms of a wear index per contact area: T_γ/A where A is the contact area, using the expression in Eq. (3):

$$\frac{T_\gamma}{A} = p(x, y) \cdot \gamma(x, y) \quad (3)$$

where T_γ/A is the scalar product of the traction (p) and the non-dimensional slip (γ) for the positions of the contact point located at (x, y) coordinates [9].

Wheels and rails may suffer damage due to wear and crack growth due to rolling contact fatigue (RCF). The phenomenon of enduring such damage differs depending on the scenarios of wheel and rail interaction [14]. This can therefore result in different types of RCF defects. Several types of RCF defects have been reviewed over many years by various authors [15–21]. The severity of RCF in railway applications depends on the numerous operational, infrastructure and wheel–rail adhesion conditions [22] that govern the elastic–plastic material behaviour triggered by rolling–sliding contact. Mainly, two models are used to estimate RCF occurrence for railway applications: the surface fatigue index model, based on the shakedown mechanism [23], and the energy dissipation model based on T-gamma [24]. Shakedown maps developed by Johnson [25] enable assessing the compressive stress limits that the material can withstand without the risk of RCF or ratcheting [26]. A shakedown analysis establishes load and traction limits, classifying the possible contact conditions into elastic shakedown, plastic shakedown, and ratcheting [27]. Thus, shakedown maps have been historically used to limit traction forces and vehicle weight or to implement wheel and rail profiles that augment the contact area to achieve an optimised minimum desirable area of wheel and rail profiles, diminishing wear and the RCF occurrence probability [28]. Modern RCF prediction studies are normally conducted using computerised multibody dynamics analyses. As RCF is not only a function of the wheel–rail normal contact force resulting from the vehicle mass, but also a function of the tangential forces caused by traction, braking, curve negotiation, and other dynamic behaviour on the wheel–rail interface [29]. Non-Hertzian wheel–rail contact models, for example, the CONTACT algorithm, and the Extended Kik-Piotrowski or Kalker Book of

Tables, are used for multibody simulation (MBS) RCF studies. Although non-Hertzian contact models are more time-consuming and computationally intense, they deliver better local vertical and tangential forces results, as they allow for generic contact shapes that produce non-elliptical contact patches as routinely occur in railway applications [30].

Although wear rates are typically low under lubricated conditions, water and lubricants may promote RCF cracks. Thus, fatigue testing usually involves lubricants [31]. However, wear and RCF are closely related such that, in some cases, severe wear may prevent the occurrence of RCF [32, 33].

Figure 1 shows the relationship among wear, wear rate, and RCF on the life of rail steel. The wheel–rail surface may fail by wear, RCF, or both. The life of the rail decreases with the increase in wear rate if only wear is considered, and this is reversed if only fatigue is considered. However, wear and RCF co-exist which creates the actual life profile of the rail shown by the bold line. The actual life above the horizontal line is the optimum life. The horizontal line intersects the actual life curve at point-A (failure by RCF) and point-B (failure by wear). The interesting observation from the figure is that, for the same material, a higher material removal rate leads to safer operation [34]. Some of the major parameters to influence the wear and RCF in railways are track structure, vehicle type, and lubrication applied [35].

While wear occurs over time on the wheel and rail contact patch by removing the superficial layer of the

bodies in contact, RCF manifests only after multiple loading cycles, when the material ductility is exhausted and microcracks appear and propagate from the wheel or rail material [27]. Hence, it can be noted that different testing approaches are required for wear and RCF phenomena. RCF testing consists of determining the presence or absence of cracks on the wheel–rail surface or subsurface after a number of loading cycles and a corresponding load condition that causes this outcome. Consequently, the result of an RCF test is a binary qualitative judgement that indicates if RCF did or did not occur on a section of the track, wheel or rail material. On the other hand, the wear rate estimated during a wear test is a quantitative value representing the wheel or rail material mass loss for a corresponding load condition over time, for example in volume loss per unit of longitudinal travel. Consequently, from the RCF perspective, this review focuses on technologies for detecting cracks on wheels, rails, or material specimens, as a relevant aspect of modern RCF testing. From the wear testing perspective, measuring mass or dimensional variations of the test specimens require less sophisticated instruments than are necessary for crack detection. Steady state wear rates do not depend on the number of cycles, and wear test runs can be extended to achieve reliable specimen mass loss or dimensional variation measurements. Then, from the wear testing perspective, this review addresses recent advances in field and laboratory wear testing approaches.

3 RCF testing

RCF testing is important to manage possible risks and reduce disastrous failures. The defects that might appear nonthreatening to the naked eye can be at a dangerous state internally. There are high-end technologies that exist for scanning and recording the internal state of various materials [36], however, methods used for the assessments of wheel and rail defect conditions are lagging to utilize those advanced technologies. As a result, the rail RCF testing approaches are still only able to provide qualitative analysis of the simplest surface defect (i.e., squats, spalls). There are few commercially available RCF testing systems [37] and most of them are not feasible for railway application

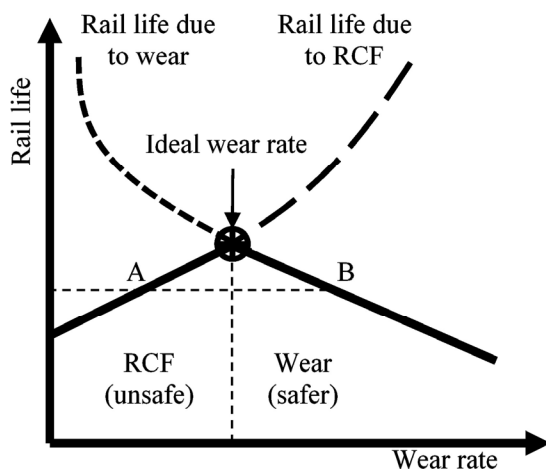


Fig. 1 Impact of wear and RCF on rail life (redrawn from Ref. [34]).

due to their low speed and manual operating requirements. On a positive note, advancement toward higher speed and machine integrated automatic systems is progressing and it seems only a matter of time before they become commercially available.

3.1 RCF testing approaches

There are several wheel–rail testing and inspection technologies available. Among them, those most commonly used for wheel–rail testing and RCF detection are based on ultrasonics, eddy current, vision, and alternating current. The competence of these technologies to detect the surface and subsurface defects are compared in Table 1 and briefly explained in the following sub-sections.

3.1.1 Ultrasonic testing (UT)

This approach transmits a beam of ultrasonic energy into the rail and the reflected energy of the beam after encountering an obstacle is detected by collection transducers. The amplitude of the reflected energy with the time stamp contains important information about the rail. In many countries, this system is usually used on Sperry trains (UTU1 and UTU2 models in the UK for example) [38]. The excessive false reading problems of UTU1 was partially addressed by setting more realistic detection thresholds and criteria in UTU2. Practically, ultrasonic rail testing systems are operated from 40 km/h up to a maximum of around 110 km/h. The third body layer is one of the major problems for this testing approach. For better results, the combination of the ultrasonic transducer approach with the pulsed eddy current method described

later has been implemented (e.g., Eurailsout [39–41], Scanmaster). To improve speed, accuracy and detection rate in rail flaw detection, many research efforts have been made to develop some innovative UT techniques. Those techniques include phased array ultrasonic testing, laser ultrasonic testing, guided wave testing, electromagnetic acoustic transducer, and acoustic emission testing.

- Phased array ultrasonic testing

Unlike the single transducer and beam used in conventional UT approaches, phased arrays use multiple ultrasonic elements and electronic time delays to create beams by constructive and destructive interference [42]. The phased array beams can be guided, scanned, swept, and focused electronically which can detect flaws in different directions, depths, and locations.

Some of the recent developments in this testing approach include a foundation work to provide information and evidence for the positioning of phased array probes in rail flaw detection [43], a hybrid array transducer combining a linear phase and a static array to precisely measure real defects in rail specimens [44], multi-element phased array technology by Speno International Company [45], the Omni-scan system by TTCI [46], and an in-parallel analysis concept also known as the fast automated angle scan technique (FAAST) which has been developed by Socomate International to address the processing in real time problem [47].

- Laser ultrasonic testing

Unlike the conventional piezoelectric ultrasonic testing, laser-based ultrasonic testing (LUT) has a remote implementation option which enables the

Table 1 Comparison of four most frequently used technologies for rail surface and subsurface testing.

Application	Surface defect	Near subsurface defect	Deep subsurface defect	Third-body layer	Couplant	Test probe position	Lift-off	Shape of defect	Inspection speed
Ultrasonic	Poor	Reasonable	Good	Problematic	Required	Close to defect center	No	Not possible	Slow
Eddy currents	Good	Reasonable	Not possible	Can detect	Not required	Wide field of view	Less than 2 mm	Not possible	Fast
Vision system	Reasonable	Not possible	Not possible	Not possible	Not required	Wide field of view	Variable	Possible	Very fast
Alternating current	Reasonable	Reasonable	Good	Can detect	Not required	Wide field of view	Up to 5 mm	Possible	Faster

ability to work in an adverse environment [48]. The pulsating laser on the solid surface creates a wave along both the longitudinal and lateral directions which can be utilized to detect defects on the surface and in the subsurface. Still, some of the existing issues with LUT are high detection cost, and low light to sound energy transformation. Some of the latest developments in this testing approach include automatic rail inspection called LURI [49], and a laser-air hybrid ultrasonic technique for rail defect inspection with a higher detection success rate [50–54].

- Guided wave testing (long-range ultrasonic)

In this ultrasonic testing (UT) technique, a volumetric ultrasonic wave is transmitted along a structure such as a rail. Long-range ultrasonics may employ a range of wave modes such as Lamb, Plate, or Rayleigh waves, but have become commonly known as the Guided Wave UT technique. An extensive review of ultrasonic guided wave technology can be found in the Ref. [55]. In rail defect detection, the ultrasonic guided wave propagates through the uneven flaws on the rail surface, reducing the screening effect of lateral cracks. Long-range ultrasonics can be effective up to 30 m from the sensor array which can be affected by the wave mode and frequency selected [56, 57]. Some recently reported research projects to inspect rail using long-range ultrasonics are available in the Refs. [58–68]. This testing approach is implemented in a hi-rail vehicle, known as Prism, by Wavesinsolids LLC in the USA [69–72] for commercial application.

- Electromagnetic acoustic transducer

In this testing approach, commonly referred to as EMAT, ultrasound is generated and detected in a magnetic or electrically conducting material. This is achieved by passing a large current pulse through an inductive coil in close proximity to a conducting surface in the existence of a strong static magnetic field, often provided by a permanent magnet [73] as shown in Fig. 2.

The advantage of using this technology is that it does not require physical coupling or acoustic matching as it is an electromagnetic coupling method that produces the ultrasound in the sample skin depth [73]. Some other advantages of this non-contact transducer technique are the ability to examine specimens with a coating layer, and the focusing and steering of the

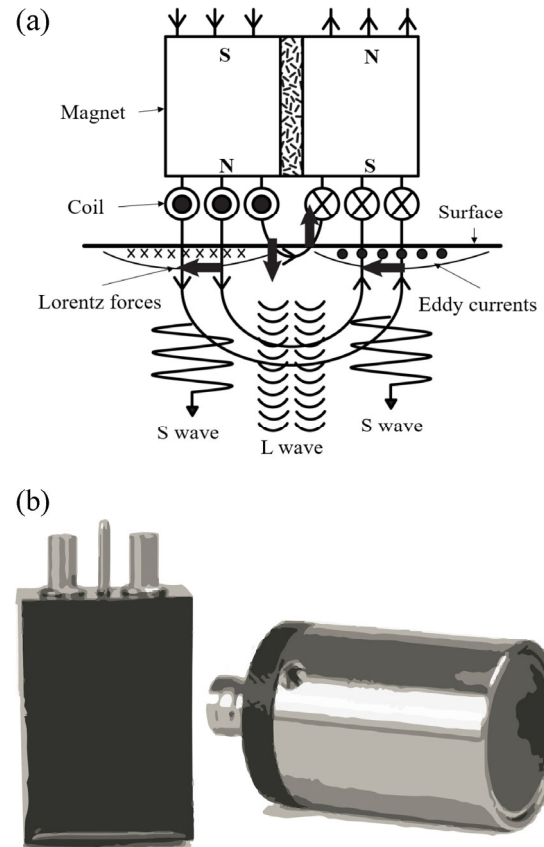


Fig. 2 EMAT: (a) typical configuration (redrawn from Ref. [73]) and (b) transducer from Olympus (redrawn from Ref. [74]).

beam at various angles to achieve defect detection from an uneven surface and subsurface.

With regard to the orientation of the magnetic field, the geometry of the coil and the physical and electrical properties of the material influence the efficiency of the EMAT. Furthermore, EMATs may be used to detect RCF cracks at high speeds but, in the case of multiple-RCF cracks, only the depth of the deepest defect may be detected [75, 76].

A commercial hi-rail vehicle including the EMAT technology has been developed by NDT Olympus and is known as RailPro. Several EMAT configurations have been used in the RailPro system to generate surface and bulk ultrasonic waves to inspect the whole section of rail [77]. The system has been tested on a special evaluation track containing several types of defects including RCF damage at inspection speeds between 5–9 km/h [77]. Advances in EMAT technology for rail inspection and quantification of RCF damage on rail have been reported by several researchers [78–84].

3.1.2 Pulsed eddy current

In this approach, alternating current is passed through an excitation coil which creates a magnetic field near the surface of the railhead and leads to the induction of eddy currents in the surface and/or near-surface layers of the metallic material under inspection [85]. Changes in the secondary magnetic field generated by the eddy currents are detected by the sensing coil. If there is a surface defect at the near-surface or on the surface, then the eddy currents cause fluctuations in the secondary magnetic field giving rise to changes in the impedance [36]. One of the main benefits of EC testing, unlike conventional ultrasonic testing, is that the EC testing sensor is not required to be in contact with the material under inspection which enables high-speed inspection capabilities. However, despite its extensive benefits, some of its weaknesses are that the EC sensor responds to undesired signal changes resulting from the variation of the material's properties, such as conductivity and permeability [86]. Also, the EC system is very susceptible to changes in the distance between the coils and the target, so special care needs to be given to avoid lift-off changes [36]. The pulsed eddy current (PEC) is an upgrade to the traditional EC method in which excitation of the inducer coil is achieved by applying a wideband of frequencies one after another in a single pulse step rather than a single frequency sinusoidal voltage [75]. The advantage of such a method is that a range of frequencies can be produced at once to obtain a range of skin depths. The PEC has been used in the railway domain as a complementary system and/or together with ultrasonic testing [41, 87–89]. Some of the recent developments of such a testing system are reported by several researchers and companies [90–99].

3.1.3 Vision system

The conventional visual inspection method performed by trained rail inspectors physically travelling along the rail track is highly subjective and places inspectors in harm's way. With the advancement in speed and resolution in camera systems, the conventional system is being replaced by an automatic vision system. The concept of such automation in the vision system is based on acquiring the video images of the rail and analyzing automatically using different image analysis software/algorithms [100, 101]. The image analysis to be

performed may range from simple pattern recognition to complex machine learning-based algorithms. Also, the analysis process depends on the speed requirement of the system. Thus, this system has been used for high-speed testing of RCF cracking. However, this system is not able to provide the information regarding internal defects and hence cannot be used as an alternative to ultrasonic testing. Some of the recent advancements of an automated vision system for RCF and rail inspection are reported by several researchers [102–109].

3.1.4 Alternating current field measurement (ACFM)

This is an electromagnetic inspection approach based on the principle that an alternating current (AC) can be induced to flow in a thin skin near the surface of any conductor. By introducing a uniform current into a section of the test component, the induced electrical current will be disturbed when there is a defect, and this influences the current to flow around the ends and down the faces of the crack as shown in Fig. 3.

The changes in the direction of the current will introduce non-uniformity to the magnetic flux which is constantly monitored using two sensors measuring the magnetic field in two directions [110].

The ACFM technique is the most recent NDT inspection method introduced in the railway industry

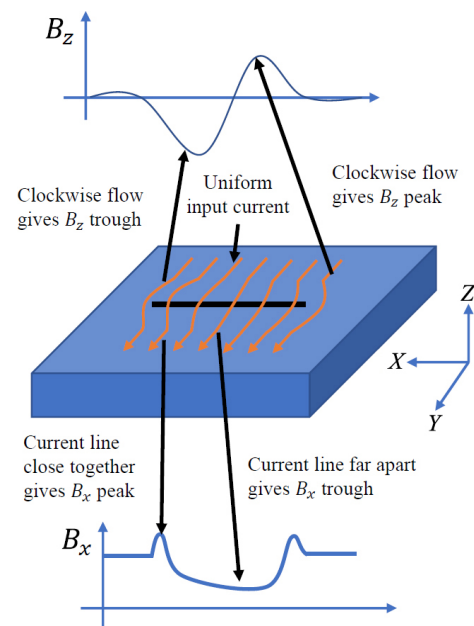


Fig. 3 Illustration of the ACFM principle (redrawn from Ref. [110]).

and some of the advantages mentioned in the literature are:

- It is a non-contact method with reduced sensitivity to lift-off (5 mm is possible without significant loss of signal) as compared to eddy current sensors that are required to be placed at a very close (<2 mm) and constant distance from the inspected surface.
- It can detect the defect and evaluate the size of the defect.
- High inspection speeds up to 80 km/h are reported.
- It can also detect a defect in the presence of dirt contamination and the third-body interfacial layer.

Although the ACFM technology was developed and patented by TSC Inspection systems initially for the routine inspection of structural welds, many research activities are being conducted to improve the technology specifically for rail inspection [111–114]. The literature claims that TSC has proven the ACFM system could detect RCF of 12 mm×2 mm in size, at 80 km/h with the lift-off of 2.3±0.5 mm [115]. Some of the recent advancements of ACFM technologies for RCF and rail inspection are reported by several researchers [116–125].

3.2 Challenges to RCF testing

As mentioned in Table 1, our literature review has shown that each RCF detection technology has some advantages and drawbacks. The ultrasonic based technologies are not that efficient in detecting surface defects and are relatively slow. However, an implementation based on this technology is being comprehensively investigated and can be expected to be developed to a practical railway application in the medium-term future. The eddy current system is offering tremendous benefits in the surface crack measurement through hand-held devices such as walking sticks and hi-rail mounted systems. More investigation is needed for detection of subsurface defects and for faster performance. The vision system can only be used for surface defect detection although higher speeds can be achieved depending on the pixel resolution required to identify the defect. All in all, successful RCF detection technology requires the integration of a range of detection technologies based on appropriately implementing their specific strengths.

4 Wear testing

There are several reasons for performing wheel-rail wear tests. Some of the major motivations are:

- Wear coefficient calculation: to develop values for use in wear models.
- Wear control: to help to select lubricants and friction modifiers.
- Wear mechanism study: to understand the wear phenomenon in different combinations of wheel-rail materials.
- Predictive tools validation: to confirm the numerical methods of wear calculation.
- Material performance benchmark: to assess new wheel-rail material and/or technologies.

Wear testing can be categorized into laboratory tests and in-service/field tests. The first type is carried out in the laboratory using a scaled or full-scale test set-up. The most common test rig setups are twin disc, pin-on-disc, reduced scale wheel-rail/roller, and full-scale wheel-rail/roller. Among these, the first two are mostly used for wear testing as they are inexpensive in comparison to wheel-rail/roller setups. Nevertheless, wheel-rail/roller setups allow for a better representation of the wheel-rail contact conditions in the field. The wear mechanism characteristics (rates and coefficients) derived from laboratory wear testing are quantified (scaled) to implement in the numerical model with the test conditions being controlled as close as possible to the real railway operational conditions [126]. The in-service/field testing performs the wear test under an actual contact condition. Most of the time such testing is performed to correlate (and validate) the results from laboratory test methods [127]. From the perspective of ease of the application and repeatability of the testing conditions, laboratory wear testing is the most popular one.

4.1 Approaches

A tool to test wear is called a wear machine (not to be confused with the tribo-machine or tribometer used for friction measurement). From the extensive literature search, dozens of wear testing apparatuses are found. The similarity in all wear machines is the involvement of two components loaded against and moving relative to each other. Table 2 shows the most popular wear testing technologies.

Table 2 Wear testing approaches.

Type	Approach	Reference	Advantages	Limitations
Laboratory	Pin-on-disc	[127–135]	<ul style="list-style-type: none"> • Low cost • Control over test parameters • Easy to prepare the test specimen • Easy data acquisition and measurement 	<ul style="list-style-type: none"> • Simplified contact geometry—pure sliding
	Twin-disc	[6, 136–146]	<ul style="list-style-type: none"> • Low cost • Control over test parameters • Easy to prepare the test specimen • Modular approach • Easy data acquisition and measurement 	<ul style="list-style-type: none"> • Simplified contact geometry—rolling contact • Hard to replicate the actual environmental conditions
	Scaled roller rig	[126, 147–149]	<ul style="list-style-type: none"> • Better representative of contact geometry 	<ul style="list-style-type: none"> • Costlier test setup and specimens
	Full scale roller rig	[9, 150–154]	<ul style="list-style-type: none"> • Actual contact geometry and contact conditions 	<ul style="list-style-type: none"> • High cost • Time-consuming • Limited control over test parameters
Field	In-service	[155–159]	<ul style="list-style-type: none"> • Actual contact geometry and real test environment 	<ul style="list-style-type: none"> • High cost • Time-consuming • Hard to obtain wear data

4.1.1 Pin-on-disc wear tester

In this type of wear tester, a pin is loaded against a flat rotating disc such that a circular wear path is created for further analysis as shown in Fig. 4. The apparatus can be used to evaluate the wear properties of materials under pure sliding conditions. From wheel and rail specimens, the disc and pin serve as either of the specimens. Various pin geometry arrangements are used as convenient.

4.1.2 Twin disc

This is the most popular wear testing approach where two discs manufactured from wheel and rail material are fixed through parallel shafts and pressed against each other under a normal load as shown in Fig. 5. In general, the wheel disc is a driving wheel

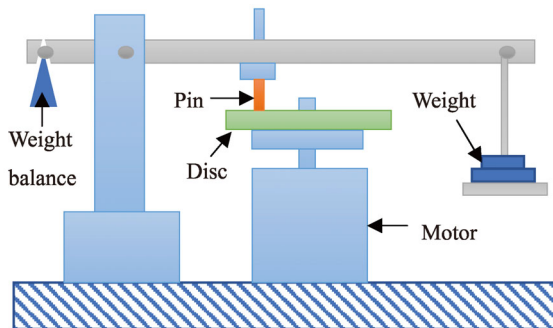


Fig. 4 Schematic of pin-on-disc wear test machine arrangement.

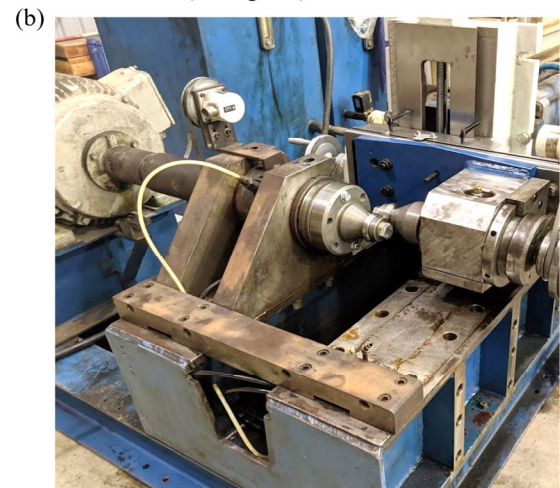
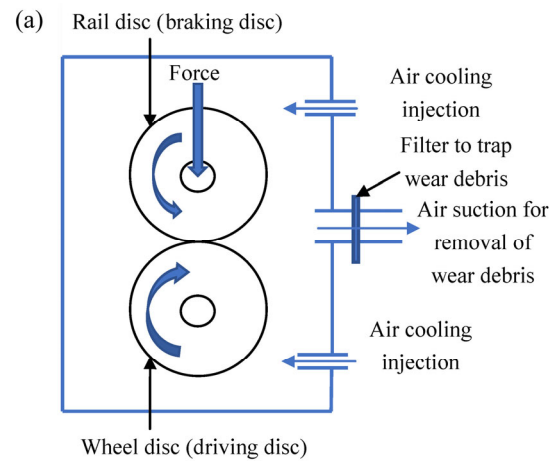


Fig. 5 Twin disc wear tester: (a) schematic, and (b) device at Centre for Railway Engineering, CQ University Australia.

driven by a motor and gear arrangement. The rotating speed is controlled by controlling the motor. Pure rolling conditions are reached when the linear speeds of the two discs are equal. For wear testing, the rolling–sliding condition is essential for which one of the discs needs to rotate slower. For that reason, the rail disc is equipped with a controlled braking system to generate a variety of slip/traction conditions.

4.1.3 Scaled roller rig

While the most common wear testing methods used with railway wheels and rails are twin disc and pin-on-disc systems, the results from these systems cannot be directly compared with the wear process occurring on a railway wheel and rail in the field as they require implementing complex scaling techniques to account for the non-linearities governing the wheel–rail contact behaviour. A few of these roller rigs are used for wear evolution and testing purposes [126, 147–149]. Typically, the results obtained from those systems require a numerical model to consider the consequences of effective slip and pressure distribution. Nevertheless, scaled roller rigs allow simulating a wide variety of vehicle–track dynamic scenarios in a safer, more controlled environment and at a fraction of the cost compared to full-scale roller rigs of full-scale field tests [160]. The main drawback of scaled roller rigs is the scaling problem, i.e., adopting a similarity strategy to effectively recreate the full-scale scenario in reduced scale laboratory conditions and subsequently transforming the measured scaled results to the full-scale case. Two of the similarity laws are used to correlate the results of scaled roller rigs with the full-scale case and include, for example, dimensional analyses or inspectional analyses to determine different scaling factors for mass, lengths, material properties, and wheel–rail/roller contact forces, among others. Reference [161] compares and provides details on various scaling strategies for scaled roller rigs from the University of Sheffield, German Aerospace Center, and the French National Institute for Transport and Safety Research. The results obtained from scaled rig experimental programs deliver insights on the material properties during the wear process under equivalent wheel–rail contact dynamics. Some of the common features of these scaled roller rigs are that they are

used to validate the numerical code determining the wear of wheel and rail profiles and they use a special profilometer to evaluate the wear of the profile.

4.1.4 Full scale roller rig

Full-scale roller rigs provide actual wheel and rail contact geometry and contact conditions. Additionally, the actual wheel and rail pieces used in the field can be used in the experimental programs performed in full-scale test rigs. Though the results can be easily transferable to represent the actual wear factors, as the results do not require complex scaling methods, the setup and operational costs are high in comparison to scaled and simplified testing methods. Nevertheless, full scale roller rigs offer less expensive and more controllable and repeatable experimental programs, compared to field tests [162]. Some relevant wear and RCF studies using full-scale roller rigs can be found in Refs. [9, 150–154].

4.1.5 Field test

This testing provides the actual wheel and rail contact geometry and the real operational environment. The field test approach requires a significant economic effort as the wear phenomenon in the field is slow in comparison to laboratory tests and it usually takes a relatively long time for wheel–rail profiles to become noticeable worn. In addition, the conditions in the field are not always easy to control as there are uncertainties introduced by weather, maintenance actions, and the different types of vehicles that operate over the same track. Some of the few field tests for wear testing in railways are discussed in Refs. [155–159]. In Refs. [155, 156], the wear tests showed that wear coefficient and sliding velocity are dependent on each other. Furthermore, the tests also establish the change of wear mechanism from mild wear to severe wear due to change in sliding velocity. In Ref. [157], the measure of rail wear is gauge face wear which is measured as lateral metal loss from that side of the high rail of the curve in contact with the wheel flange. On the other hand, the wheel tread wear is assessed as change in flange height for both powered and trailing wheels in Ref. [158]. The field test results are the best way to develop and validate a comprehensive wear model which can be easily used in combination

with other numerical simulations as performed in Ref. [159]. However, wear testing in the actual field creates enormous difficulties in obtaining the wear data along with a huge cost. Field testing is also time-consuming because each passage of the wheel propagates changes in the surface by a range of a few nano-meters [163]. The difficulties increase if a variety of different rolling stock is in use on the same railway network.

4.2 Selection of input parameters for scaled wear testing

In scaled wear testing and mapping, when using the T_γ/A wear model approach, the major parameters to consider are wear rate and T_γ/A . Varying contact pressure and slip is required to represent a sufficient range of T_γ to represent the full range of operating scenarios which may be informed by multibody dynamic simulations of the rail vehicle. Thus, it is necessary to obtain the full range of contact conditions and parameters from multibody dynamic simulations

of the rail vehicles before performing the wheel-rail wear test. The necessary parameters are elliptical contact patch size, maximum contact pressure, and sliding length. The Hertzian calculation in the elliptical contact case are shown in Table 3.

To represent the contact conditions and parameters in scaled testing (especially in twin disc tests), the Hertzian calculations of these parameters assuming the two contacting bodies as cylindrical in shape need to be considered. The equivalent calculations of the contact parameters are provided in Table 4.

Wear test machines have a limited maximum normal load capacity. Thus, the scaling of the specimen is influenced by the capacity of the test machine and the maximum required contact pressure.

4.3 Major wear measurement parameters

Wear measurement is conducted to determine the quantity of materials removed (i.e., worn off) after a wear test. The wear test resembles a portion of the service period in the real world. The wear measurement

Table 3 Hertzian elliptical contact equations (adapted from Ref. [164]).

Reduced radius	Contact area dimensions	Maximum contact pressure	Average contact pressure	Contact pressure distribution
$\frac{1}{R'} = \frac{1}{R_x} + \frac{1}{R_y}$	$a = \sqrt{\frac{3k^2 E(k) PR'}{\pi E^*}}$	$p_o = \frac{3P}{2\pi ab}$	$p_{avg} = \frac{P}{\pi ab}$	$p(x, y) = p_o \sqrt{1 - \frac{x^2}{a^2} - \frac{y^2}{b^2}}$
$\frac{1}{R_x} = \frac{1}{R_{1x}} + \frac{1}{R_{2x}}$	$b = \sqrt{\frac{3E(k) PR'}{\pi E^*}}$			
$\frac{1}{R_y} = \frac{1}{R_{1y}} + \frac{1}{R_{2y}}$				

where:

k is the ellipticity parameter ($k = a/b$) and $E(k)$ is an elliptic integral of the second kind. The elliptic integral may be obtained from tables of mathematical data. Alternatively, an approximate solution is given by

$$k = 1.0339 \left(\frac{R_y}{R_x} \right)^{0.6360} \quad \text{and} \quad E = 1.0003 \left(\frac{0.5968 R_x}{R_y} \right)$$

The reduced elastic modulus, E^* , is given by

$$\frac{1}{E^*} = \frac{1 - \nu_1^2}{E_1} + \frac{1 - \nu_2^2}{E_2}$$

where:

ν_1 and ν_2 are the Poisson's ratios of the contacting bodies '1' and '2', respectively.

E_1 and E_2 are the elastic moduli of the contacting bodies '1' and '2', respectively.

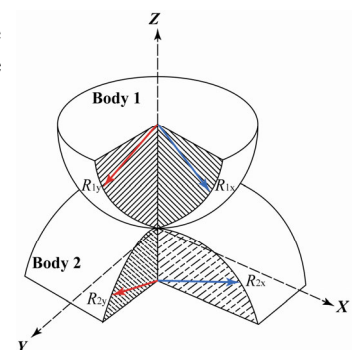
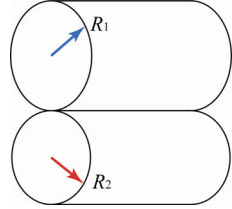


Table 4 Hertzian line contact equations (adapted from Ref. [164]).

Reduced radius	Contact area dimensions	Maximum contact pressure	Average contact pressure	Contact pressure distribution
$\frac{1}{R} = \frac{1}{R_1} + \frac{1}{R_2}$	$b = \sqrt{\frac{4P'R'}{\pi E^*}}$	$p_o = \frac{2P'}{\pi b}$	$p_{avg} = \frac{P'}{2b}$	$p(x) = p_o \sqrt{1 - \frac{x^2}{b^2}}$

where:
b is the half width of the contact strip (m).
P' is the load per unit length (N/m).



can be expressed either as weight (mass) loss, volume loss, or linear dimension variation depending on the purpose of the test, the geometry and size of the test specimens, the type of wear, and the availability of a measurement resource. Commonly, the mass loss is measured using a precision balance. The volume loss is evaluated by measuring the wear depth and/or assessing the cross-sectional area using a dedicated microscope. Linear dimension variation is determined through surface profiling/scanning. Brief explanations of the major wear measurement parameters are also presented in Table 5.

4.3.1 Mass loss

- This is a convenient method for wear measurement.
- Measured by a precision balance.
- Good for irregular and unsymmetrical worn surfaces.
- The difference in weight before and after the test represents the weight loss caused by wear and is expressed in gram (g) or microgram (µg).

4.3.2 Volume loss

- Wear volume loss is usually determined from the wear track (trace) depth, length, width and/or profile depending on the geometry of the nature of wear.
- A surface profilometer (e.g., a stylus type, or a microscope with a scale) is used for the measurement.
- The wear volume loss is expressed in mm³ or µm³.
- It allows for better evaluation of wear among materials having different densities.
- In the case of complex/irregular wear track, mass loss may be calculated first, and the volume loss is determined for the uniform materials with a known density.

4.3.3 Linear dimension loss

- This is a simplified wear measuring approach and provides an initial estimation of the wear track.
- This approach is combined with the volume loss approach for better results.

Table 5 Major wear measurement parameters.

Measurement type	Measurement method	Advantages	Wear unit
Mass loss	<ul style="list-style-type: none"> • Measured by a precision balance. • Can be calculated from volume if the density is known. 	<ul style="list-style-type: none"> • Useful if the work surface is irregular and unsymmetrical. 	µg
Volume loss	<ul style="list-style-type: none"> • Determined from the wear track (/trace) depth, length, width and/or profile depending on the geometry of the nature of wear. • A surface profilometer is used for the measurement. • Can be calculated from mass loss if the density is known. 	<ul style="list-style-type: none"> • Allows for better evaluation of wear among materials having different densities. 	mm ³
Linear dimension loss	<ul style="list-style-type: none"> • A surface profilometer (e.g., a stylus type, or a microscope with scale) is used for the measurement. 	<ul style="list-style-type: none"> • Simplified wear measuring approach and provides an initial estimation of the wear track. 	µm

- A surface profilometer (e.g., a stylus type, or a microscope with scale) is used for the measurement.
- The linear dimension loss is expressed in mm or μm .
- Since wear testing involves the removal of material from specimens, careful consideration of parameters before, during, and after the test are important. Some other parameters required to be measured for wear testing recommended by Lewis et al. [164] are presented in Table 6.

4.4 Presenting wear results

The three wear models presented in Section 2 propose different wear outputs: the T-gamma wear model produces a wear number (T_γ) [5]; Archard's wear model uses wear volume [7, 8] and the USFD wear model computes a wear rate [9, 10]. When using the Archard's wear model (Eq. (2)), the wear volume is a function of the wear coefficient K , which is related to the sliding velocity and contact pressure and is determined using a wear map as shown in Fig. 6(a). The Archard's wear coefficient map is built through experimental programs. The USFD wear model (Eq. (3)) determines the wear rate as a function of T_γ/A , as shown in Fig. 6(b). The USFD wear map classifies the computed wear rate into a piece-wise-linear pattern covering three wear regimes: mild (K1), intermediate (K2), and severe (K3). While the USFD wear rate is linearly dependent on the T_γ/A for wear regimes of mild and severe, it is constant for the whole intermediate region. The wear regimes and transitions are determined through experimental programs whose results are typically implemented subsequently in MBS analyses to estimate wear volumes for specific vehicle-track operational scenarios. Wear rate versus T_γ/A plots are ideal for comparing the wear behavior of different types of wheel and rail materials and their combinations as well as the general trends of specific materials wear performance. Alternatively, wear coefficients presented as contour map (Fig. 6(c)) or a 3D graph (Fig. 6(d)) permit studying the individual contributions of the contact pressure or sliding speed to the wear volume and wear regime transitions [10]. These outcomes allow railway operators to carefully optimize vehicle weight or traction limits while extending the life of wheel and rails for specific material combinations. Table 7 presents the main parameters used to study wear results.

Table 6 Parameters required to measure wear test (taken from Ref. [164]).

Pre-test measurement	
• Mass (after cleaning)	• Surface hardness
• Roughness	• Sub-surface hardness
• Sub-surface image	• Surface image
During-test measurement	
• Friction	• Slip
• Load (/pressure)	• Test cycle (/length)
• Intermittent wear (either stopping the test or using appropriate technology)	• Contact temperature
	• Temperature and humidity
	• Unusual specimen behavior (e.g., change in noise, change of specimen surface)
Post-test measurement	
• Mass (after cleaning)	• Surface hardness
• Roughness	• Sub-surface hardness gradient
• Third-body layer thickness	• Surface image
• Third-body layer composition	• Sub-surface deformation
	• Wear derbies characteristics

4.5 Challenges to wear testing

While scaled wear tests are better in terms of cost, control over test parameters, and test repeatability, some issues need to be carefully considered and mitigated before final implementation.

- Scaling the wear value

There have been two methods implemented in scaling the wear value. The first approach is comparing the wear from a reduced scale with the full-scale using T_γ values based on the principle that, for the same T_γ value, the mass loss should be the same [10, 154, 164, 165]. The second approach is to validate laboratory wear coefficients results with data from full-scale tests complemented with numerical studies [9, 166–169].

- Specimen and contact geometry

In field trials, the actual wheel and rail are used, producing actual contact geometries and contact conditions. While scaled wheel–rail/roller approaches use specimens that try to replicate the wheel and rail/roller material properties, however they do not achieve exact field conditions. Depending on the size of the disc required, the specimen can be prepared from the actual wheel and rail materials (if the disc is the size of a railhead) or a comparable material. The specimen for the twin disc is obtained from the actual

Table 7 Calculation of wear and its related parameters.

Parameter	Calculation	Unit
Wear amount, W	mass loss or volume loss or linear dimension loss	μg , mm^3 , μm
Sliding length, L	number of cycle $\times 2\pi \times$ nominal disc-radius	m
Contact area, A	$\pi \times$ major semiaxis(a) \times minor semiaxis(b)	mm^2
Wear rate	$\frac{\text{wear amount}}{\text{sliding length} \times \text{contact area}}$	$\mu\text{g}/\text{m}/\text{mm}^2$
Slip	$\left(\frac{\omega_2 \times (R_2) - \omega_1 \times (R_1)}{\omega_2 \times (R_2) + \omega_1 \times (R_1)} \right) \cdot 200\%$	—
Traction coefficient, μ	$\frac{\text{tangential force}}{\text{normal force}}$	—
T_y/A	$\frac{\text{traction coefficient} \times \text{normal force} \times \text{slip}}{\text{area of contact ellipse}}$	N/mm^2
Wear coefficient	$\frac{\text{wear amount} \times \text{material hardness}}{\text{sliding length} \times \text{normal force}}$	—

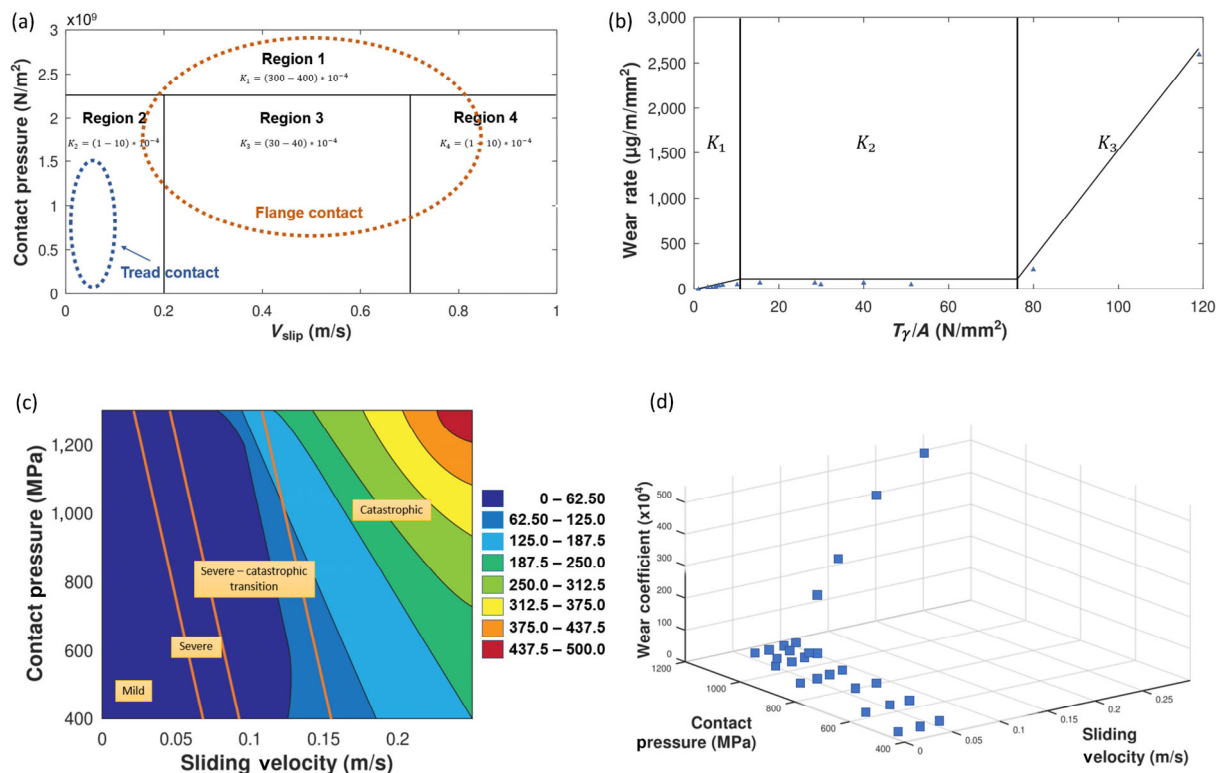


Fig. 6 Example of quantitative representations of wear : (a) Archard wear coefficient map (redrawn from Refs. [7, 8]); (b) wear rate and wear regimes map (redrawn from Ref. [11]), (c) 2D contour map of the wear coefficient (redrawn from Ref. [10]), and (d) 3D points graph of wear coefficient (redrawn from Ref. [10]).

wheel and rail. Both pin-on-disc and twin disc machine tests have simplified contact geometry.

- Test cycles
Extended number of cycles are an important yet

challenging factor in laboratory wear testing because it is correlated with high temperature generation, oxide formation, and reduced contact pressure between the wheel and rail/roller contact. During the test, the

same rolling contact area of a specimen comes into interaction repetitively, creating excessive heat [170]. As a result, thermal softening of the material occurs which increases the wear rate. The wear rate continues to rise to attain a peak and gradually drops to reach a steady-state wear as shown in Fig. 7.

In addition, the oxide formation in the contact creates a denser third body layer which is unlikely to be evident in the real field scenario [172–174]. Additionally, the contact pressure can be changed when the specimen is worn due to continuous interaction. Thus, it is necessary to select the number of test cycles (l /length) as per the relevant technical requirement. An extensive insight has been provided on test cycle issues in Ref. [171]. And the importance of maintaining the temperature at the level of the actual contact and how it is performed is elaborated upon in Refs. [142,158,170].

- Normal load calculation

Another challenge is to determine the normal load for the test. The normal load is directly proportional to the maximum pressure required in the test (refer to Table 4). The maximum pressure required is derived from the multibody dynamic simulation. For the given maximum pressure, the normal load is calculated from the equation provided in Table 4.

- Environmental conditions

Environmental conditions influence the wear rates and wear mechanisms observed in the field. An extensive review of how the environmental conditions affect the wear between wheel and rail was conducted

in Ref. [175]. The authors observed that the wear rate decreased with increasing ambient humidity or the presence of water in the wheel–rail interface. Additionally, the authors highlighted the influence of low temperatures on the wear mechanisms. Ma et al. [176] observed that wear rates doubled at very low temperatures ($-40\text{ }^{\circ}\text{C}$, $-30\text{ }^{\circ}\text{C}$, $-15\text{ }^{\circ}\text{C}$), compared to room temperature tests using a twin-disc experimental setup. Hence, appropriate selection and control of environmental conditions is a challenging aspect to consider when performing a wear test in a laboratory setup.

5 Discussion and conclusions

This study starts with the explanation of relationships and differences between RCF and wear during wheel–rail interaction. It is essential to understand such distinctions because these parameters have often mistakenly been used as interchangeably.

Moreover, from the extensive analysis of the different RCF testing approaches, it can be observed that each testing approach has some benefits. Thus, the key take-away message for conducting RCF testing is to select the proper approach as per the necessity of the test conditions, project budget, timelines, and previous investigations performed in comparable wheel–rail materials. It is also advisable for complex test conditions to implement more than one approach simultaneously.

Wear and RCF are complex phenomena in the railway environment, influenced by numerous tribological parameters that include wheel-profile geometry, third body materials, environmental conditions, vehicle dynamics, and friction conditions that vary along space and time, among others. Field tests allow the most accurate results, considering all the tribological parameters, but are expensive, offer poor repeatability, and are time consuming as wear and RCF can only be quantified after they have occurred. Laboratory scaled and full-scale wear and RCF tests offer less expensive alternatives, with more repeatability and control but a reduced spectrum of tribological parameters in terms of vehicle dynamics, wheel–rail contact behaviour, and environmental conditions. Nevertheless, the results of laboratory

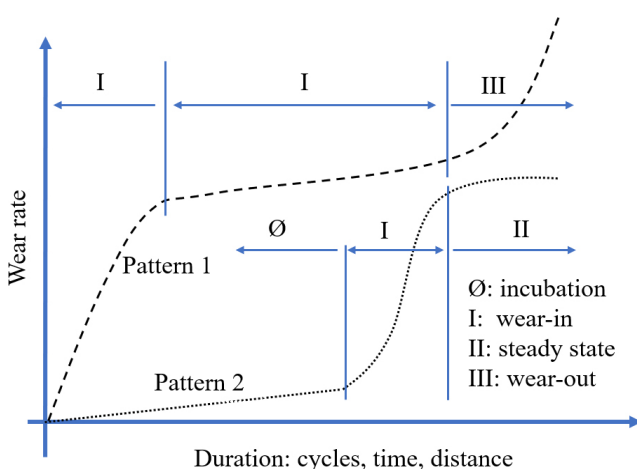


Fig. 7 Two most common non-linear sliding wear behavior patterns (redrawn from Ref. [171]).

experimental programs can be scaled and expanded through numerical multibody dynamics studies. Furthermore, recent advances in high performance computing allow conducting numerical experimental programs that consider vast amounts of particular combinations of vehicle–track operational and tribological parameters that were previously unviable. Additionally, the reduction in costs of technology and recent advances in digital manufacturing, sensors, and vision systems now permit laboratory and field test that are less expensive and at the same time produce more wear and RCF data. All the RCF defect detection technologies analysed in this review can be implemented in the field as well as in laboratory setups.

For a wear and RCF experimental program to produce results that are truly representative of the conditions in the field, it is necessary to use the same wheel–rail material combinations along with equipment that allows reproducing the friction and normal loads that occur in normal operation. Furthermore, the literature reviewed did not find a precise and defined method for determining the values of the variables that govern the test (number of cycles, normal load, speed, torque/traction force) according to a specific vehicle configuration–track layout combination. Further research is required to develop a method that allows condensing a train trip (or series of train trips) for a single railway vehicle, considering traction, braking, lateral coupler forces, speed tables, and other parameters affecting the vehicle’s dynamics. Such a tool would allow more advanced wear and RCF studies involving laboratory experimental programs that evaluate the performance of wheel–rail material combinations taking into account all the possible operating slip and contact pressure conditions for specific track layouts–vehicle combinations.

From the analytical study of the recent wear testing approaches, the key take-away messages to conducting the testing are as follows:

- Specimen material selection: obtain the specimens for the actual wheel and rail if possible. If not, the best representative material could be used.
- Specimen temperature: maintain the usual operational temperature using cooling airflow and/or pausing the test.

- Environmental condition: though it is relatively difficult to replicate the environmental conditions, it is recommended to attempt to do so as much as possible.
- Contact condition representation: replicate the most representative contact conditions by testing across different scenarios to generate ample data.
- Number of test cycles: use enough test cycles to represent different stages of wear.
- Test type selection: shifting from field trials to reduced scale tests decreases the experimental complexity, but creates less representative contact conditions. Additionally, there are many other parameters as shown in Fig. 8 to consider in making the testing approach fit for purpose.

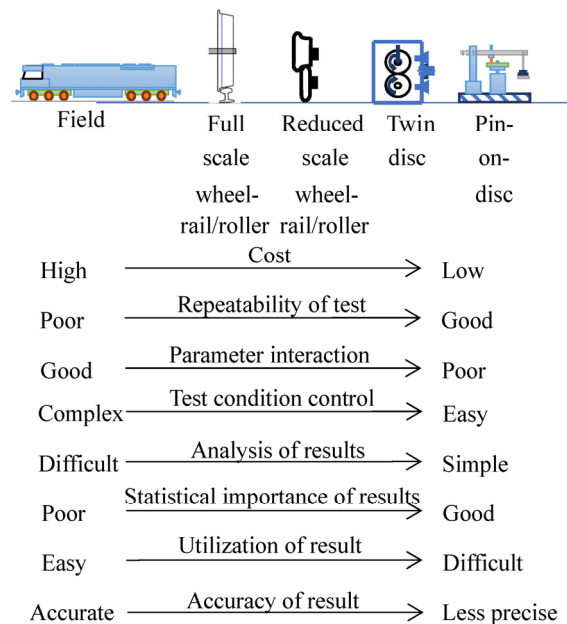


Fig. 8 Classification of wear testing approaches according to their degree of applicability and interaction.

Acknowledgements

The authors would like to acknowledge the support of the Australasian Centre for Rail Innovation (ACRI) and their industry partners that have contributed to the HH27 ‘Wear Simulation Development - Stage 1’ project. Dr Qing Wu is the recipient of an Australian Research Council Discovery Early Career Award (project number DE210100273) funded by the Australian Government. Tim McSweeney, Adjunct Research Fellow, Centre for Railway Engineering

is thankfully acknowledged for his assistance with proofreading.

Declaration of competing interest

The authors have no competing interests to declare that are relevant to the content of this article.

Open Access This article is licensed under a Creative Commons Attribution 4.0 International License, which permits use, sharing, adaptation, distribution and reproduction in any medium or format, as long as you give appropriate credit to the original author(s) and the source, provide a link to the Creative Commons licence, and indicate if changes were made.

The images or other third party material in this article are included in the article's Creative Commons licence, unless indicated otherwise in a credit line to the material. If material is not included in the article's Creative Commons licence and your intended use is not permitted by statutory regulation or exceeds the permitted use, you will need to obtain permission directly from the copyright holder.

To view a copy of this licence, visit <http://creativecommons.org/licenses/by/4.0/>.

References

- [1] Kragelsky I V, Dobychin M N, Kombatov V S. *Friction and Wear: Calculation Methods*. Elsevier, 1982.
- [2] Varenberg M. Towards a unified classification of wear. *Friction* **1**(4): 333–340 (2013)
- [3] Lontin K, Khan M. Interdependence of friction, wear, and noise: A review. *Friction* **9**(6): 1319–1345 (2021)
- [4] Wu Q, Spiriyagin M, Sun Y, Cole C. Parallel co-simulation of locomotive wheel wear and rolling contact fatigue in a heavy haul train operational environment. *Proc Inst Mech Eng F J Rail Rapid Transit* **235**(2): 166–178 (2021)
- [5] Pearce T G, Sherratt N D. Prediction of wheel profile wear. *Wear* **144**(1–2): 343–351 (1991)
- [6] Bolton P J, Clayton P. Rolling–sliding wear damage in rail and tyre steels. *Wear* **93**(2): 145–165 (1984)
- [7] Jendel T. Prediction of wheel profile wear—Comparisons with field measurements. *Wear* **253**(1–2): 89–99 (2002)
- [8] Enblom R. On simulation of uniform wear and profile evolution in the wheel-rail contact. *DiVA - Academic Archive On-line* (2006)
- [9] Braghin F, Lewis R, Dwyer-Joyce R S, Bruni S. A mathematical model to predict railway wheel profile evolution due to wear. *Wear* **261**(11–12): 1253–1264 (2006)
- [10] Lewis R, Olofsson U. Mapping rail wear regimes and transitions. *Wear* **257**(7–8): 721–729 (2004)
- [11] Lewis R, Dwyer-Joyce R S, Olofsson U, Pombo J, Ambrosio J, Pereira M, Ariaudo C, Kuka N. Mapping railway wheel material wear mechanisms and transitions. *Proc Inst Mech Eng F J Rail Rapid Transit* **224**: 125–137 (2010)
- [12] Bevan A, Molyneux-Berry P, Eickhoff B, Burstow M. Development and validation of a wheel wear and rolling contact fatigue damage model. *Wear* **307**(1–2): 100–111 (2013)
- [13] Lewis R, Olofsson U. Basic tribology of the wheel-rail contact. In *Wheel-Rail Interface Handbook*. Amsterdam: Elsevier, 2009: 34–57
- [14] Huang Y B, Shi L B, Zhao X J, Cai Z B, Liu Q Y, Wang W J. On the formation and damage mechanism of rolling contact fatigue surface cracks of wheel/rail under the dry condition. *Wear* **400–401**: 62–73 (2018)
- [15] Cannon D F, Edel K O, Grassie S L, Sawley K. Rail defects: An overview. *Fatigue Fract Eng Mater Struct* **26**(10): 865–886 (2003)
- [16] Ekberg A. Rolling contact fatigue of railway wheels—A parametric study. *Wear* **211**(2): 280–288 (1997)
- [17] Ekberg A, Åkesson B, Kabo E. Wheel/rail rolling contact fatigue—Probe, predict, prevent. *Wear* **314**(1–2): 2–12 (2014)
- [18] Grassie S L. Rolling contact fatigue on the British railway system: Treatment. *Wear* **258**(7–8): 1310–1318 (2005)
- [19] Magel E, Kalousek J. Identifying and interpreting railway wheel defects. In *Proceedings of International Heavy Haul Association Conference on Freight Car Trucks/Bogies*, Montreal, Canada, 1996.
- [20] Soleimani H, Moavenian M. Tribological aspects of wheel-rail contact: A review of wear mechanisms and effective factors on rolling contact fatigue. *Urban Rail Transit* **3**(4): 227–237 (2017)
- [21] Ma L, He C G, Zhao X J, Guo J, Zhu Y, Wang W J, Liu Q Y, Jin X S. Study on wear and rolling contact fatigue behaviors of wheel/rail materials under different slip ratio conditions. *Wear* **366–367**: 13–26 (2016)
- [22] Six K, Mihalj T, Trummer G, Marte C, Krishna V V, Hossein-Nia S, Stichel S. Assessment of running gear performance in relation to rolling contact fatigue of wheels and rails based on stochastic simulations. *Proc Inst Mech Eng F J Rail Rapid Transit* **234**(4): 405–416 (2020)
- [23] Ekberg A, Kabo E, Andersson H. An engineering model for prediction of rolling contact fatigue of railway wheels. *Fatigue Fract Eng Mater Struct* **25**(10): 899–909 (2002)

- [24] Burstow M C. Whole life rail model application and development for RSSB (T115)—Continued development of an RCF damage parameter. London: Rail Standards and Safety Board, 2004.
- [25] Johnson K L. *Contact Mechanics*. Cambridge University Press, 2008.
- [26] Krabbenhøft K, Lyamin A V, Sloan S W. Bounds to shakedown loads for a class of deviatoric plasticity models. *Comput Mech* 39(6): 879–888 (2007)
- [27] Bernal E, Spiryagin M, Vollebregt E, Oldknow K, Stichel S, Shrestha S, Ahmad S, Wu Q, Sun Y, Cole C. Prediction of rail surface damage in locomotive traction operations using laboratory-field measured and calibrated data. *Eng Fail Anal* 135: 106165 (2022)
- [28] Hasan N. Shakedown limits and uses in railroad engineering. *J Mater Civ Eng* 31(11): 04019282 (2019)
- [29] Vollebregt E, Six K, Polach O. Challenges and progress in the understanding and modelling of the wheel-rail creep forces. *Veh Syst Dyn* 59(7): 1026–1068 (2021)
- [30] Liu B B, Bruni S. Comparison of wheel-rail contact models in the context of multibody system simulation: Hertzian versus non-Hertzian. *Veh Syst Dyn* 60(3): 1076–1096 (2022)
- [31] Alwahdi F. Wear and rolling contact fatigue of ductile materials. Ph.D. Thesis. The University of Sheffield, 2004
- [32] Gallardo Hernandez E A. Wheel and rail contact simulation using a twin disc tester. Ph.D. thesis. University of Sheffield, 2009.
- [33] Turnia J, Sinclair J, Perez J, A review of wheel wear and rolling contact fatigue. *Proc Inst Mech Eng F J Rail Rapid Transit* 221: 271–289 (2007)
- [34] Kapoor A, Fletcher D I, Franklin F J. The role of wear in enhancing rail life. *Tribol Ser* 41: 331–340 (2003)
- [35] Meng Y G, Xu J, Jin Z M, Prakash B, Hu Y Z. A review of recent advances in tribology. *Friction* 8(2): 221–300 (2020)
- [36] Papaalias M P, Roberts C, Davis C L. A review on non-destructive evaluation of rails: State-of-the-art and future development. *Proc Inst Mech Eng F J Rail Rapid Transit* 222: 367–384 (2008)
- [37] Innotrack. D4.4.1 – Rail Inspection Technologies, INNOTRACK Project Number TIP5-CT-2006-031415, 2008. <http://www.innotrack.net/IMG/pdf/d441.pdf>.
- [38] Clark R. Rail flaw detection: Overview and needs for future developments. *NDT E Int* 37(2): 111–118 (2004)
- [39] Bezemer L, Weel T, Flach G, Hanspach G, Thomas H-M. Device for guiding eddy current sensors along railway tracks for a non destructive inspection of the rail surface. EP 1 547 898 B1, 2006.
- [40] Pohl R, Erhard A, Montag H J, Thomas H M, Wüstenberg H. NDT techniques for railroad wheel and gauge corner inspection. *NDT E Int* 37(2): 89–94 (2004)
- [41] Thomas H M, Heckel T, Hanspach G. Advantage of a combined ultrasonic and eddy current examination for railway inspection trains. *Insight Non Destr Test Cond Monit* 49(6): 341–344 (2007)
- [42] Moles M. Advances in phased array ultrasonic technology applications. Olympus NDT Adv Pract NDT Ser 491 (2007) <http://scholar.google.com/scholar?hl=en&btnG=Search&q=intitle:Advances+in+Phased+Array+Ultrasonic+Technology+Applications#3>.
- [43] Utrata D. Exploring enhanced rail flaw detection using ultrasonic phased array inspection. *AIP Conf Proc* 615(1): 1813–1818 (2002)
- [44] Wooh S C, Wang J Y. Nondestructive characterization of defects using a novel hybrid ultrasonic array sensor. *NDT E Int* 35(3): 155–163 (2002)
- [45] Alaix R. High speed rail testing with phased array probes. In *7th World Congr Railw Res*, Montreal, Canada, 2006.
- [46] Garcia G, Zhang J. Application of ultrasonic phased arrays for rail flaw inspection. Department of Transportation, Federal Railroad Administration, Office of Research and Development, Washington, DC, U.S., 2006.
- [47] Coperet P. FAAST—Fast Automated Angle Scan Technique. In *ECNDT 2006 Conf*, 2006: 1–9.
- [48] Bond L J. *Laser Ultrasonics, Techniques and Applications*. CRC Press, 1991.
- [49] Nielsen S A, Bardenshtein A L, Thommesen A, Stenum B. Automatic laser ultrasonics for rail inspection. In *16th World Conf Non-Destructive Test*, 2004.
- [50] Kenderian S, Cerniglia D, Djordjevic B B, Garcia G. Laser-air hybrid ultrasonic technique for dynamic railroad inspection applications. *Insight Non Destr Test Cond Monit* 47(6): 336–340 (2005)
- [51] Kenderian S, Djordjevic B B, Cerniglia D, Garcia G. Dynamic railroad inspection using the laser-air hybrid ultrasonic technique. *Insight Non Destr Test Cond Monit* 48(6): 336–341 (2006)
- [52] Lanza di Scalea F, Rizzo P, Coccia S, Bartoli I, Fateh M, Viola E, Pascale G. Non-contact ultrasonic inspection of rails and signal processing for automatic defect detection and classification. *Insight Non Destr Test Cond Monit* 47(6): 346–353 (2005)
- [53] Montinaro N, Epasto G, Cerniglia D, Guglielmino E. Laser ultrasonics inspection for defect evaluation on train wheel. *NDT E Int* 107: 102145 (2019)
- [54] Cavuto A, Martarelli M, Pandarese G, Revel G M, Tomasini E P. Train wheel diagnostics by laser ultrasonics. *Measurement* 80: 99–107 (2016)

- [55] Ling en hong, Abdul Rahim R H. A review on ultrasonic guided wave technology. *Aust J Mech Eng* **18**(1): 32–44 (2020)
- [56] Wilcox P, Evans M, Pavlakovic B, Alleyne D, Vine K, Cawley P, Lowe M. Guided wave testing of rail. *Insight* **45**(6): 413–420 (2003)
- [57] Di Scalea F L, Bartoli I, Rizzo P, Fateh M. High-speed defect detection in rails by noncontact guided ultrasonic testing. *Transportation Research Record* **1916**(1): 66–77 (2005)
- [58] Loveday P W. Guided wave inspection and monitoring of railway track. *J Nondestruct Eval* **31**(4): 303–309 (2012)
- [59] Coccia S, Bartoli I, Salamone S, Phillips R, di Scalea F L, Fateh M, Carr G. Noncontact ultrasonic guided wave detection of rail defects. *Transportation Research Record* **2117**(1): 77–84 (2009)
- [60] Campos-Castellanos C, Gharaibeh Y, Mudge P, Kappatos V. The application of long range ultrasonic testing (LRUT) for examination of hard to access areas on railway tracks. In *5th IET Conf Railw Cond Monit Non Destr Test RCM*, 2011.
- [61] Wang S J, Chen X Y, Jiang T, Kang L. Electromagnetic ultrasonic guided waves inspection of rail base. In *2014 IEEE Far East Forum on Nondestructive Evaluation/Testing*, Chengdu, China, 2014.
- [62] Coccia S, Bartoli I, Marzani A, Lanza di Scalea F, Salamone S, Fateh M. Numerical and experimental study of guided waves for detection of defects in the rail head. *NDT E Int* **44**(1): 93–100 (2011)
- [63] Teidj S, Khamlich A, Driouach A. Generating guided waves for detection of transverse type-defects in rails. *Appl Mech Mater* **772**: 355–358 (2015)
- [64] Gharaibeh Y, Sanderson R, Mudge P, Ennaceur C, Balachandran W. Investigation of the behaviour of selected ultrasonic guided wave modes to inspect rails for long-range testing and monitoring. *Proc Inst Mech Eng F J Rail Rapid Transit* **225**(3): 311–324 (2011)
- [65] Pathak M, Alahakoon S, Spiriyagin M, Cole C. Rail foot flaw detection based on a laser induced ultrasonic guided wave method. *Measurement* **148**: 106922 (2019)
- [66] Rizzo P, Cammarata M, Bartoli I, di Scalea F L, Salamone S, Coccia S, Phillips R. Ultrasonic guided waves-based monitoring of rail head: Laboratory and field tests. *Adv Civ Eng* **2010**: 1–13 (2010)
- [67] Mariani S, Nguyen T V, Zhu X, Sternini S, Lanza di Scalea F, Fateh M, Wilson R. Non-contact ultrasonic guided wave inspection of rails: Next generation approach. In *2016 Joint Rail Conference*, Columbia, South Carolina, USA, 2016.
- [68] Mariani S, Nguyen T, Phillips R R, Kijanka P, Lanza di Scalea F, Staszewski W J, Fateh M, Carr G. Noncontact ultrasonic guided wave inspection of rails. *Struct Health Monit* **12**(5–6): 539–548 (2013)
- [69] Rose J L, Lee C M, Hay T R, Cho Y, Park I K. Rail inspection with guided waves. In *J Acoust. Soc. Am.*, Auckland, New Zealand, 2006: 733–740.
- [70] Lee C M, Rose J L, Cho Y. A guided wave approach to defect detection under shelling in rail. *NDT E Int* **42**(3): 174–180 (2009)
- [71] Rose J L, Avioli M J, Mudge P, Sanderson R. Guided wave inspection potential of defects in rail. *NDT E Int* **37**(2): 153–161 (2004)
- [72] Lee C M, Rose J L, Luo W, Cho Y H. A computational tool for defect analysis in rail with ultrasonic guided waves. *Key Eng Mater* **321–323**: 784–787 (2006)
- [73] Maxfield B. *Electromagnetic Acoustic Transducers, Second Edition*. Springer Japan, Tokyo, 2003.
- [74] Huang S L, Wang S, Li W B, Wang Q. Electromagnetic acoustic transducer. In *Electromagnetic Ultrasonic Guided Waves*. Singapore: Springer Singapore, 2016: 1–42
- [75] Rowshandel H. The development of an autonomous robotic inspection system to detect and characterise rolling contact fatigue cracks in railway track, The University of Birmingham, 2014. <http://etheses.bham.ac.uk/4821/>.
- [76] Dixon S, Edwards R S, Jian X. Inspection of rail track head surfaces using electromagnetic acoustic transducers (EMATs). *Insight* **46**(6): 326–330 (2004)
- [77] Chahbaz A, Brassard M, Pelletier A. Mobile inspection system for rail integrity assessment. In *15th World Conf. NDT*, Rome, Italy, 2013: 1–6.
- [78] Zhang K, Yi P, Li Y, Hui B, Zhang X. A new method to evaluate surface defects with an electromagnetic acoustic transducer. *Sensors (Basel)* **15**(7): 17420–17432 (2015)
- [79] Yi Z, Wang K C, Kang L, Zhai G F, Wang S J. Rail flaw detection system based on electromagnetic acoustic technique. In *5th IEEE Conference on Industrial Electronics and Applications*, Taichung, Taiwan, China, 2010: 211–215
- [80] Li Y Q, Li C, Su R L, Zhai G F, Wang K C. Unidirectional line-focusing shear vertical wave EMATs used for rail base center flaw detection. In *2016 IEEE Far East NDT New Technology & Application Forum (FENDT)*, Nanchang, China, 2016: 99–102
- [81] Vishesh S, Srinath M, Sreeram S, Jayanth P, Samarth Bharadwaj D D, Venkatachalapathi S S. Advanced monitoring of rail cracks using LASER-EMAT system. *IJARCCCE* **5**(12): 413–416 (2016)
- [82] Petcher P A, Potter M D G, Dixon S. A new electromagnetic acoustic transducer (EMAT) design for operation on rail. *NDT E Int* **65**: 1–7 (2014)

- [83] Lu C, Men P, Li L X. An experimental study of EMAT ultrasonic surface waves modes in railhead. *Int J Appl Electromagn Mech* **33**(3–4): 1127–1133 (2010)
- [84] Santos R, Jiménez J A, Boyero C, Romero A, García V, Syed A, Hernández F, López B. New EMAT solutions for the railway industry. In *12th ECNDT Conf*, Gothenburg, Sweden, 2018.
- [85] Bowler N. *Eddy-Current Nondestructive Evaluation*. Springer New York, 2019.
- [86] Rajamäki J, Vippola M, Nurmikolu A, Viitala T. Limitations of eddy current inspection in railway rail evaluation. *Proc Inst Mech Eng F J Rail Rapid Transit* **232**(1): 121–129 (2018)
- [87] Szugs T, Krüger A, Jansen G, Beltman B, Gao S, Mühlmeier H, Ahlbrink R. Combination of ultrasonic and eddy current testing with imaging for characterization of rolling contact fatigue. In *19th World Conf. Non-Destructive Test.*, Munich, Germany, 2016: 1–8.
- [88] Rockstroh B, Kappes W, Walte F, Kröning M, Bessert S, Seitz R, Hintze H, Pieper W, Schümann N, Heilmann P. Ultrasonic and eddy-current inspection of rail wheels and wheel set axles. In *17th World Conf. Nondestruct. Test.*, Shanghai, China, 2008: 25–28.
- [89] Gao S, Szugs T, Inspection E, Ahlbrink R. Use of combined railway inspection data sources for characterization of rolling contact fatigue. In *12th ECNDT Conf.*, 2018.
- [90] Thomas H M, Dey A, Heyder R. Eddy Current test method for early detection of rolling contact fatigue (RCF) in rails. *Insight Non Destr Test Cond Monit* **52**(7): 361–365 (2010)
- [91] Wilson J, Tian G Y, Mukriz I, Almond D. PEC thermography for imaging multiple cracks from rolling contact fatigue. *NDT E Int* **44**(6): 505–512 (2011)
- [92] Peng J P, Tian G Y, Wang L, Zhang Y, Li K J, Gao X R. Investigation into eddy current pulsed thermography for rolling contact fatigue detection and characterization. *NDT E Int* **74**: 72–80 (2015)
- [93] Feng L F, Peng J P, Zhang K, Bai J, Gao X R. Research on eddy current pulsed thermography for Squats in railway. In *Proceedings of the 2018 International Conference on Quantitative InfraRed Thermography*. QIRT Council, 2018: 586–593.
- [94] Zhu J Z, Wu J B, Tian G Y, Gao Y I. Detection and reconstruction of rolling contact fatigue cracks using eddy current pulsed thermography. In *2018 IEEE Far East NDT New Technology & Application Forum (FENDT)*, Xiamen, China, 2018.
- [95] Zhu J Z, Withers P J, Wu J B, Liu F, Yi Q J, Wang Z J, Tian G Y. Characterization of rolling contact fatigue cracks in rails by eddy current pulsed thermography. *IEEE Trans Ind Inform* **17**(4): 2307–2315 (2021)
- [96] Song Z L, Yamada T, Shitara H, Takemura Y. Detection of damage and crack in railhead by using eddy current testing. *J Electromagn Anal Appl* **3**(12): 546–550 (2011)
- [97] Vaibhav T, Balasubramaniam K, Thomas R, Chandra Bose A. (2016) Eddy Current thermography for rail inspection. In *Proceedings of the 2016 International Conference on Quantitative InfraRed Thermography*. QIRT Council, 2016: 862–869.
- [98] Peng J P, Tian G Y, Wang L, Gao X R, Zhang Y, Wang Z Y. (2014) Rolling contact fatigue detection using eddy current pulsed thermography. In *2014 IEEE Far East Forum on Nondestructive Evaluation/Testing*, Chengdu, China, 2014.
- [99] Zhang K, Peng J P, Yang K, Gao X R, Zhang Y, Peng C Y, Tian G Y. Research on eddy current pulsed thermography for rolling contact fatigue crack detection and quantification in wheel tread. In *2016 18th International Wheelset Congress (IWC)*, Chengdu, China, 2016.
- [100] Chenariyan Nakhaee M, Hiemstra D, Stoelinga M, van Noort M. The recent applications of machine learning in rail track maintenance: A Survey. In *Lect. Notes Comput. Sci. (Including Subser. Lect. Notes Artif. Intell. Lect. Notes Bioinformatics)*, 2019: 91–105.
- [101] Santur Y, Karaköse M, Akin E. A new rail inspection method based on deep learning using laser cameras. In *2017 International Artificial Intelligence and Data Processing Symposium (IDAP)*, Malatya, Turkey. IEEE, 2017: 1–6
- [102] Li Q Y, Ren S W. A real-time visual inspection system for discrete surface defects of rail heads. *IEEE Trans Instrum Meas* **61**(8): 2189–2199 (2012)
- [103] Min Y Z, Xiao B Y, Dang J W, Yue B, Cheng T D. Real time detection system for rail surface defects based on machine vision. *EURASIP J Image Video Process* **2018**(1): 1–11 (2018)
- [104] Yuan H, Chen H, Liu S W, Lin J, Luo X. A deep convolutional neural network for detection of rail surface defect. In *2019 IEEE Vehicle Power and Propulsion Conference (VPPC)*, Hanoi, Vietnam, 2019.
- [105] Bodini I, Petrogalli C, Mazzù A, Pasinetti S, Kato T, Makino T. A vision-based approach for rolling contact fatigue evaluation in twin-disc tests on a railway wheel steel. *Tribol Mater Surf Interfaces* **15**(2): 92–101 (2021)
- [106] Liu B L, Brigham J C, Jun H, Yuan X C, Hu H L. Roll contact fatigue defect recognition using computer vision and deep convolutional neural networks with transfer learning. *Eng Res Express* **1**(2): 025018 (2019)
- [107] Raza Rizvi A, Rauf Khan P, Ahmad S. Crack detection in railway track using image processing. *Int J Adv Res Ideas Innov Technol* **3**: 489–496 (2017)

- [108] Bodini I, Sansoni G, Lancini M, Pasinetti S, Docchio F. Feasibility study of a vision system for on-line monitoring of rolling contact fatigue tests. *J Phys: Conf Ser* **778**: 012007 (2017)
- [109] Li J Y, Liang J K, Chen G B, Yang Y. Research on key control technology of intelligent rolling contact fatigue test facility. *J Control Sci Eng* **2020**: 1–11 (2020)
- [110] M. Lugg, D. Topp, Recent Developments and Applications of the ACFM Inspection Method and ACSM Stress Measurement Method, EandT. (2006) 1–14.
- [111] Topp D, Smith M. Application of the ACFM inspection method to rail and rail vehicles. *Insight Non Destr Test Cond Monit* **47**(6): 354–357 (2005)
- [112] Howitt M. Bombardier brings ACFM into the rail industry. *Insight Non-Destructive Test Con Monit* **44**: 379–382 (2002)
- [113] Shen J. Responses of alternating current field measurements (ACFM) to rolling contact fatigue cracks in railway rails. Ph.D. Thesis. Coventry (U.K.): University of Warwick, 2017.
- [114] Shen J, Zhou L, Warnett J, Williams M. The influence of rcf crack propagation angle and crack shape on the ACFM signal. In *19th World Conf. Non Destr. Test.*, 2016: 1–9.
- [115] Transalley. The rail industry in the region. <https://www.transalley.com/en/overview/the-rail-industryin-the-region>, 2015.
- [116] Papaalias M P, Lugg M C, Roberts C, Davis C L. High-speed inspection of rails using ACFM techniques. *NDT E Int* **42**(4): 328–335 (2009)
- [117] Papaalias M P, Lugg M. Detection and evaluation of rail surface defects using alternating current field measurement techniques. *Proc Inst Mech Eng F J Rail Rapid Transit* **226**(5): 530–541 (2012)
- [118] Ph Papaalias M, Roberts C, Davis C L, Blakeley B, Lugg M. Further developments in high-speed detection of rail rolling contact fatigue using ACFM techniques. *Insight Non Destr Test Cond Monit* **52**(7): 358–360 (2010)
- [119] Ph Papaalias M, Roberts C, Davis C L, Lugg M, Smith M. Detection and quantification of rail contact fatigue cracks in rails using ACFM technology. *Insight Non Destr Test Cond Monit* **50**(7): 364–368 (2008)
- [120] Nicholson G L, Rowshandel H, Hao X J, Davis C L. Measurement and modelling of ACFM response to multiple RCF cracks in rail and wheels. *Ironmak Steelmak* **40**(2): 87–91 (2013)
- [121] Nicholson G L, Kostryzhev A G, Hao X J, Davis C L. Modelling and experimental measurements of idealised and light-moderate RCF cracks in rails using an ACFM sensor. *NDT E Int* **44**(5): 427–437 (2011)
- [122] Nicholson G L, Davis C L. Modelling of the response of an ACFM sensor to rail and rail wheel RCF cracks. *NDT E Int* **46**: 107–114 (2012)
- [123] Nicholson G, Rowshandel H, Papaalias M, Davis C, Roberts C. Sizing and tomography of rolling contact fatigue cracks in rails using NDT technology-potential for high speed application. In *9th World Conf. Railw. Res.*, Lille, France, 2011.
- [124] Rowshandel H, Nicholson G L, Davis C L, Roberts C. A robotic approach for NDT of RCF cracks in rails using an ACFM sensor. *Insight* **53**(7): 368–376 (2011)
- [125] Rowshandel H, Papaalias M, Roberts C, Davis C. Development of autonomous ACFM rail inspection techniques. *Insight Non Destr Test Cond Monit* **53**(2): 85–89 (2011)
- [126] Kumar S, Prasanna Rao D L. Wheel-rail contact wear, work, and lateral force for zero angle of attack—A laboratory study. *J Dyn Syst Meas Control* **106**(4): 319–326 (1984)
- [127] Robles Hernández F C, Demas N G, Gonzales K, Polycarpou A A. Correlation between laboratory ball-on-disk and full-scale rail performance tests. *Wear* **270**(7–8): 479–491 (2011)
- [128] Conshohocken W. Standard test method for wear testing with a pin-on-disk apparatus. ASTM G99-17.
- [129] Sundh J, Olofsson U, Sundvall K. Seizure and wear rate testing of wheel-rail contacts under lubricated conditions using pin-on-disc methodology. *Wear* **265**(9–10): 1425–1430 (2008)
- [130] Lyu Y Z, Zhu Y, Olofsson U. Wear between wheel and rail: A pin-on-disc study of environmental conditions and iron oxides. *Wear* **328–329**: 277–285 (2015)
- [131] Prates Ferreira de Almeida L, Entringer Falqueto L, Goldenstein H, Cesar Bozzi A, Scandian C. Study of sliding wear of the wheel flange-rail gauge corner contact conditions: Comparative between cast and forged steel wheel materials. *Wear* **432–433**: 102894 (2019)
- [132] Faccoli M, Petrogalli C, Ghidini A. A pin-on-disc study on the wear behaviour of two high-performance railway wheel steels. *Tribol Lett* **65**(4): 1–7 (2017)
- [133] Lee K M, Polycarpou A A. Wear of conventional pearlitic and improved bainitic rail steels. *Wear* **259**(1–6): 391–399 (2005)
- [134] Mezrin A M. Determining local wear equation based on friction and wear testing using a pin-on-disk scheme. *J Frict Wear* **30**(4): 242–245 (2009)
- [135] Zhu Y, Sundh J, Olofsson U. A tribological view of wheel-rail wear maps. *Int J Railw Tech* **3**(3): 79–91 (2013)
- [136] Krause H, Poll G. Wear of wheel-rail surfaces. *Wear* **113**(1): 103–122 (1986)
- [137] Zhou L, Wang W J, Hu Y, Marconi S, Meli E, Ding H H, Liu Q Y, Guo J, Rindi A. Study on the wear and damage

- behaviors of hypereutectoid rail steel in low temperature environment. *Wear* **456–457**: 203365 (2020)
- [138] Wang W J, Zhong W, Guo J, Liu Q Y, Zhu M H, Zhou Z R. Investigation on rolling contact fatigue and wear properties of railway rails. *Proc Inst Mech Eng Part J J Eng Tribol* **223**(7): 1033–1039 (2009)
- [139] Deters L, Proksch M. Friction and wear testing of rail and wheel material. *Wear* **258**(7–8): 981–991 (2005)
- [140] Wang W J, Lewis R, Yang B, Guo L C, Liu Q Y, Zhu M H. Wear and damage transitions of wheel and rail materials under various contact conditions. *Wear* **362–363**: 146–152 (2016)
- [141] Garnham J E, Beynon J H. Dry rolling-sliding wear of bainitic and pearlitic steels. *Wear* **157**(1): 81–109 (1992)
- [142] Lewis R, Dwyer-Joyce R S. Wear mechanisms and transitions in railway wheel steels. *Proc Inst Mech Eng J J Eng Tribol* **218**: 467–478 (2004)
- [143] Hasan S M, Chakrabarti D, Singh S B. Dry rolling/sliding wear behaviour of pearlitic rail and newly developed carbide-free bainitic rail steels. *Wear* **408–409**: 151–159 (2018)
- [144] Mazzù A, Solazzi L, Lancini M, Petrogalli C, Ghidini A, Faccoli M. An experimental procedure for surface damage assessment in railway wheel and rail steels. *Wear* **342–343**: 22–32 (2015)
- [145] Santa J F, Cuervo P, Christoforou P, Harmon M, Beagles A, Toro A, Lewis R. Twin disc assessment of wear regime transitions and rolling contact fatigue in R400HT–E8 pairs. *Wear* **432–433**: 102916 (2019)
- [146] Donzella G, Faccoli M, Mazzù A, Petrogalli C, Roberti R. Progressive damage assessment in the near-surface layer of railway wheel-rail couple under cyclic contact. *Wear* **271**(1–2): 408–416 (2011)
- [147] Bosso N, Zampieri N. Experimental and numerical simulation of wheel-rail adhesion and wear using a scaled roller rig and a real-time contact code. *Shock Vib* **2014**: 1–14 (2014)
- [148] Jin Y, Ishida M, Namura A. Experimental simulation and prediction of wear of wheel flange and rail gauge corner. *Wear* **271**(1–2): 259–267 (2011)
- [149] Shebani A, Iwnicki S. Prediction of wheel and rail wear under different contact conditions using artificial neural networks. *Wear* **406–407**: 173–184 (2018)
- [150] Marte C, Six K, Trummer G, Dietmaier P, Kienberger A, Stock R, Fischmeister E, Oberhauser A, Rosenberger M. Application of a new wheel-rail contact model to wear simulations—Validation with wear measurements. In *Proc. IAVSD2011 - 22nd Int Symp Dyn Veh Roads Tracks*, 2011: 1–6.
- [151] Cantini S, Cervello S. The competitive role of wear and RCF: Full scale experimental assessment of artificial and natural defects in railway wheel treads. *Wear* **366–367**: 325–337 (2016)
- [152] McEwen I J, Harvey R F. Full-scale wheel-on-rail wear testing: comparisons with service wear and a developing theoretical predictive method. *Lubr Eng* **41**: 80–88 (1985)
- [153] Stock R, Pippin R. RCF and wear in theory and practice—The influence of rail grade on wear and RCF. *Wear* **271**(1–2): 125–133 (2011)
- [154] Eadie D T, Elvidge D, Oldknow K, Stock R, Pointner P, Kalousek J, Klausner P. The effects of top of rail friction modifier on wear and rolling contact fatigue: Full-scale rail–wheel test rig evaluation, analysis and modelling. *Wear* **265**(9–10): 1222–1230 (2008)
- [155] Olofsson U, Telliskivi T. Wear, plastic deformation and friction of two rail steels—A full-scale test and a laboratory study. *Wear* **254**(1–2): 80–93 (2003)
- [156] Olofsson U, Nilsson R. Surface cracks and wear of rail: A full-scale test on a commuter train track. *Proc Inst Mech Eng F J Rail Rapid Transit* **216**(4): 249–264 (2002)
- [157] Steele R K. Observations of in-service wear of railroad wheels and rails under conditions of widely varying lubrication. *S L E Trans* **25**(3): 400–409 (1982)
- [158] Walia M S, Vernersson T, Lundén R, Blennow F, Meinel M. Temperatures and wear at railway tread braking: Field experiments and simulations. *Wear* **440–441**: 203086 (2019)
- [159] Auciello J, Ignesti M, Malvezzi M, Meli E, Rindi A. Development and validation of a wear model for the analysis of the wheel profile evolution in railway vehicles. *Veh Syst Dyn* **50**(11): 1707–1734 (2012)
- [160] Bernal E, Spiriyagin M, Cole C. Wheel flat analogue fault detector verification study under dynamic testing conditions using a scaled bogie test rig. *Int J Rail Transp* **10**(2): 177–194 (2022)
- [161] Bosso N, Allen P D, Zampieri N. Scale testing theory and approaches. In *Handbook of Railway Vehicle Dynamics*. CRC Press, 2019: 825–867
- [162] Allen P D, Zhang W H, Liang Y R, Zeng J, Jung H, Meli E, Ridolfi A, Rindi A, Heller M, Koch J. Roller rigs. In *Handbook of Railway Vehicle Dynamics*. CRC Press, 2019: 761–823
- [163] Fletcher D I, Franklin F J, Kapoor A. Rail surface fatigue and wear. In *Wheel-Rail Interface Handbook*. Amsterdam: Elsevier, 2009: 280–310
- [164] Lewis R, Magel E, Wang W J, Olofsson U, Lewis S, Slatter T, Beagles A. Towards a standard approach for the wear testing of wheel and rail materials. *Proc Inst Mech Eng F J Rail Rapid Transit* **231**(7): 760–774 (2017)
- [165] Buckley-Johnstone L, Harmon M, Lewis R, Hardwick C,

- Stock R. A comparison of friction modifier performance using two laboratory test scales. *Proc Inst Mech Eng F J Rail Rapid Transit* **233**: 201–210 (2019)
- [166] Ignesti M, Innocenti A, Marini L, Meli E, Rindi A. Development of a model for the simultaneous analysis of wheel and rail wear in railway systems. *Multibody Syst Dyn* **31**(2): 191–240 (2014)
- [167] Innocenti A, Marini L, Meli E, Pallini G, Rindi A. Development of a wear model for the analysis of complex railway networks. *Wear* **309**(1–2): 174–191 (2014)
- [168] Pombo J, Ambrósio J, Pereira M, Lewis R, Dwyer-Joyce R, Ariaudo C, Kuka N. A study on wear evaluation of railway wheels based on multibody dynamics and wear computation. *Multibody Syst Dyn* **24**(3): 347–366 (2010)
- [169] Pombo J, Ambrósio J, Pereira M, Lewis R, Dwyer-Joyce R, Ariaudo C, Kuka N. Development of a wear prediction tool for steel railway wheels using three alternative wear functions. *Wear* **271**(1–2): 238–245 (2011)
- [170] Gallardo-Hernandez E A, Lewis R, Dwyer-Joyce R S. Temperature in a twin-disc wheel/rail contact simulation. *Tribol Int* **39**(12): 1653–1663 (2006)
- [171] Blau P J. How common is the steady-state? The implications of wear transitions for materials selection and design. *Wear* **332–333**: 1120–1128 (2015)
- [172] Descartes S, Desrayaud C, Niccolini E, Berthier Y. Presence and role of the third body in a wheel-rail contact. *Wear* **258**(7–8): 1081–1090 (2005)
- [173] Lewis R, Dwyer-Joyce R S, Lewis S R, Hardwick C, Gallardo-Hernandez E A. Tribology of the wheel-rail contact: The effect of third body materials. *Int J Railw Tech* **1**(1): 167–194 (2012)
- [174] Zhu Y. The influence of iron oxides on wheel-rail contact: A literature review. *Proc Inst Mech Eng F J Rail Rapid Transit* **232**(3): 734–743 (2018)
- [175] Zhu Y, Wang W J, Lewis R, Yan W Y, Lewis S R, Ding H H. A review on wear between railway wheels and rails under environmental conditions. *J Tribol* **141**(12): 1–13 (2019)
- [176] Ma L, Shi L B, Guo J, Liu Q Y, Wang W J. On the wear and damage characteristics of rail material under low temperature environment condition. *Wear* **394–395**: 149–158 (2018)



Sundar SHRESTHA. He is research officer at the Centre for Railway Engineering, Central Queensland University, Australia. He received his master degree of engineering in 2015 from Rosenheim University of Applied Sciences, Germany. The master thesis was completed as a collaboration research project between the University and BOSCH

Germany. He worked as vision system engineer before starting his Ph.D. in 2017. He received his Ph.D. degree in railway braking in 2021 from Central Queensland University. Prior to his current role, he has involved in research and consultancy projects as research assistant. His research interests include mechatronics, automation engineering, contact mechanics, and railway vehicle dynamics.



Maksym SPIRYAGIN. He is the deputy director of the Centre for Railway Engineering and a professor of Engineering at Central Queensland University, Australia. He received his Ph.D. degree in the field of railway transport in 2004. Professor Spiryagin's involvement in academia and railway industry projects includes many years of research experience in locomotive design and

traction, rail vehicle dynamics, contact mechanics, wear, mechatronics, and the development of complex systems using various approaches. He has published four books, including "Design and simulation of rail vehicles" in 2014 and "Design and simulation of heavy haul locomotives and trains" in 2017, and he has more than two hundred other scientific publications and twenty patents as one of the inventors. Professor Spiryagin is a chartered professional engineer and RPEQ in Australia and a chartered engineer in the UK.



Esteban BERNAL. He is a senior research officer at the Centre For railway Engineering, Central Queensland University, Australia. During his doctoral dissertation he

studied innovative on-board condition monitoring technologies for railway vehicles. Additionally, he has participated in research and consultancy projects involving vehicle dynamics simulations and wheel–rail wear and damage studies.



Qing WU. He is a research fellow at the Centre for Railway Engineering, Central Queensland University, Australia. He has a Ph.D. degree in the topic of heavy haul trains, a master of engineering in the topic of heavy haul locomotives and a bachelor of engineering in the topic of heavy

haul wagons. He has more than 100 publications in the railway domain. He is a recipient of an Australian Research Council Discovery Early Career Award (project number DE210100273) funded by the Australian Government. His current research interests include train system dynamics, wagon/locomotive dynamics, track dynamics, data analysis, multi-objective optimisations, and parallel computing.



Colin COLE. He is the director of the Centre for Railway Engineering at Central Queensland University, Australia. He has worked in the Australian rail industry since 1984, starting with six years in mechanized track maintenance for Queensland Railways. Since then, he has focused on a research and consulting career involving work on track maintenance, train and wagon dynamics, train

control technologies, and the development of on-board devices. He has been extensively engaged with industry via the past nationally funded Rail CRC programs and the Australasian Centre for Rail Innovation. His Ph.D. was in longitudinal train dynamics modelling. He has authored and/or co-authored over two hundred technical papers, two books, numerous commercial research and consulting reports, and has developed two patents relating to in-cabin locomotive technologies.